The Origin of Complex Dynamics: A Tale of Two Systems

A. Bergeon[1], E. Knobloch[2]

Summary

Complex dynamics found in (a) natural doubly-diffusive convection, and (b) surface tension-driven convection in a binary liquid mixture using a combination of numerical continuation and direct numerical simulation in three dimensions are linked to the presence of global bifurcations in the phase space of the governing field equations.

Introduction

We describe and compare the mechanisms behind the presence of complex dynamics in two convection systems: natural doubly-diffusive convection and surface tension-driven convection in three-dimensional enclosures. We use numerical branch-following techniques [2],[3] to follow branches of steady states through parameter space, together with their stability properties. We search for regimes in which none of these simple states is stable, and then use direct numerical simulation [4] to determine the behavior of the system in this regime. Our systems illustrate two different mechanisms for generating such a "stability gap". In the former it comes about via the onset of a three-dimensional instability that is absent in a strictly two-dimensional formulation. In the latter the gap is created by changing the horizontal cross-section of the container from square to slightly rectangular, i.e., via forced symmetry-breaking. In each case we provide a geometrical interpretation for the presence of complex dynamics in the stability gap.

Natural doubly diffusive convection

Natural doubly diffusive convection, i.e., convection driven by a horizontal concentration and temperature gradients perpendicular, displays a wealth of dynamical behavior. We assume that the wall at $x = 0$ is maintained at temperature $\Delta T > 0$ and concentration $\Delta C > 0$ above those imposed at $x = L$, and measure the relative importance of the temperature and concentration gradients by the buoyancy ratio $N = \rho_C \Delta C / \rho_T \Delta T$, where $\rho_T \equiv \partial\rho/\partial T < 0$, $\rho_C \equiv \partial\rho/\partial C > 0$. The dimensionless governing equations are

$$\frac{\partial \mathbf{u}}{\partial t} = -(\mathbf{u}\cdot\nabla)\,\mathbf{u} - \nabla p + \nabla^2\mathbf{u} + Gr(T + NC)\mathbf{e}_z, \qquad \nabla.\mathbf{u} = 0, \tag{1}$$

$$\frac{\partial T}{\partial t} = -(\mathbf{u}\cdot\nabla)\,T + \frac{1}{Pr}\nabla^2 T, \qquad \frac{\partial C}{\partial t} = -(\mathbf{u}\cdot\nabla)\,C + \frac{1}{Sc}\nabla^2 C, \tag{2}$$

where $Gr \equiv g\rho_T \Delta T L^3/\nu^2$ is the Grashof number, and Pr, Sc are the Prandtl and Schmidt numbers. Here g is the gravitational acceleration, and ν the kinematic viscosity. The heat

[1]IMFT UMR CNRS 5502 - Université Paul Sabatier UFR MIG, 118, route de Narbonne, 31062 Toulouse, France

[2]Department of Applied Mathematics, University of Leeds, Leeds LS2 9JT, UK

and mass fluxes vanish along the boundaries $y = 0, A_y$ and $z = 0, A_z$, and $\mathbf{u} \equiv (u, v, w) = 0$ on all walls.

When $N = -1$ the problem has the conduction solution $\mathbf{u} = \theta = \Sigma = 0$, where $T = 1 - x + \theta(x, y, z)$, $C = 1 - x + \Sigma(x, y, z)$. With the given boundary conditions the equations for $\mathbf{u}$, θ, Σ are invariant under the two operations

$$S_y : (x, y, z) \to (x, A_y - y, z), \qquad (u, v, w, \theta, \Sigma) \to (u, -v, w, \theta, \Sigma), \tag{3}$$

$$S_\Delta : (x, y, z) \to (1 - x, y, A_z - z), \qquad (u, v, w, \theta, \Sigma) \to (-u, v, -w, -\theta, -\Sigma). \tag{4}$$

Thus S_y is a reflection in the plane $y = A_y/2$ while S_Δ is a rotation by π about the line $x = 1/2$, $z = A_z/2$. It follows that the equations are also invariant under the operation $S_\Delta \circ S_y = S_y \circ S_\Delta \equiv S_C$, corresponding to a point symmetry with respect to the center of the container. These symmetries constitute the symmetry group D_2. If S is a nontrivial element of D_2 and $\mathbf{e}$ is an eigenvector of the linearized problem, then $S\mathbf{e} = \pm\mathbf{e}$, i.e., the instability either respects or breaks the symmetry S. As a result each neutral stability curve is characterized by a particular symmetry. In particular, if $S\mathbf{e} = \mathbf{e}$ for all $S \in D_2$, the generic bifurcation from the conduction state is transcritical. In contrast, if one of the reflections in D_2 is broken, the bifurcation is a pitchfork. In the bifurcation diagrams these facts are indicated using the notation T_j for the jth transcritical bifurcation from the conduction state, and P_j for the jth pitchfork bifurcation. The diagrams show $W_M \equiv |w|_{\max}$, i.e., the maximum of the absolute value of the vertical velocity in the enclosure, as a function of the Grashof number. Thus two distinct branches of solutions, unrelated by any of the problem symmetries, emerge from points labeled T_j. In contrast, the two solutions emerging from points P_j are related by the broken symmetry and so have identical values of W_M at fixed Gr; consequently only a single solution branch emerges from each P_j.

When $Pr = 1$, $Sc = 11$ and $A_y = 1$, $A_z = 2.5$ (fig. 1a) the first instability, at $Gr_{P_1} = 997.5$, is a subcritical pitchfork bifurcation. The resulting unstable branch terminates in a pitchfork bifurcation at $Gr_{S_2} = 959.2$ on the subcritical branch emanating from a transcritical bifurcation at T_1 ($Gr_{T_1} = 1045$). After S_2 the latter branch undergoes a second pitchfork bifurcation at S_1 ($Gr_{S_1} = 770$), and then a saddle-node bifurcation at $Gr_{SN} = 679$, but remains unstable throughout. The supercritical branch emanating from T_1 is initially once unstable and undergoes two Hopf bifurcations before terminating on the conduction state at T_2. Thus over the entire range of parameter values explored the only stable steady solutions are those located on the branch created at S_1, associated with *longitudinal* rolls, between the two Hopf bifurcations H_1 ($Gr_{H_1} = 1267$) and H_2 ($Gr_{H_2} = 1568$). The "stability" gap $Gr_{P_1} < Gr < Gr_{H_1}$ is created when S_1 moves down past SN [3].

The bifurcation at Gr_{H_1} is supercritical and so produces stable small amplitude oscillations in $Gr < Gr_{H_1}$. In contrast the bifurcation at H_2 is subcritical and leads to large amplitude oscillations. These persist down to $Gr \approx 936.5$ and up to the largest values of Gr explored ($Gr > 3000$), coexisting with the small amplitude oscillations in the interval $1085 < Gr < Gr_{H_1} \approx 1267$. In order to detect the symmetry of the corresponding flow we construct three indicators of symmetry breaking: for a generic point M inside the

container we compute the quantities $I_y = w(M) - w(S_y(M))$, $I_\Delta = w(M) + w(S_\Delta(M))$ and $I_C = w(M) + w(S_C(M))$ as a function of time. If any of these indicators vanishes identically the flow has the corresponding symmetry. Using this technique we show that all the oscillations found for $A_z = 2.5$ are S_C-symmetric. Figure 1b shows the time evolution of I_y and $w(M)$ when $Gr = 936.5$, while fig. 1c shows a plot of I_y against $w(M)$. The figure shows that the oscillation is almost heteroclinic, spending a long time near two fixed points, labeled A and B. Figure 1c shows that these fixed points are S_y-symmetric, in addition to having the symmetry S_C of the oscillation. Thus both correspond to D_2-symmetric steady states. Both solutions lie on the subcritical steady state branch emanating from T_1 with the solution B located on the lower part of the branch and A on the upper part. At this value of Gr ($Gr_{S_1} < Gr < Gr_{S_2}$) the solution B is unstable with respect to D_2-symmetric perturbations but no other. A solution starting near B will therefore follow the unstable manifold of B which takes it to A. This solution is stable with respect to D_2-symmetric perturbations since it lies above SN but because it also lies above the point S_1 it is unstable with respect to perturbations breaking S_y (and hence S_Δ as well). This is confirmed in fig. 1b which shows that $I_y > 0$ once the solution escapes from A. The one-dimensional unstable manifold of A then takes the system back to B; during this phase the flow is dominated by longitudinal rolls. As Gr decreases to Gr^* the oscillation becomes more and more burst-like, before losing stability in a saddle-node bifurcation prior to a *heteroclinic* bifurcation at $Gr = Gr^*$, $936 < Gr^* < 936.5$ [3].

Similar behavior occurs at other values of the aspect ratio and does not require the presence of the conduction state $N = -1$. Figure 2 shows examples for $A_x = A_y = 1$ and (left) $N = -0.99$, (right) $N = -1.007$, for comparison with the $N = -1$ case in [3]. Both cases exhibit complex dynamics for reasons identical to those described above.

Surface tension-driven convection

We next turn to binary mixtures with a free but undeformable surface, in which convection is driven by temperature and concentration-dependent surface tension [2],[4]. As a result gravity can be ignored, and the bifurcation parameter becomes the Marangoni number instead of the Grashof number. We suppose that the system is heated from above by a constant heat flux $-q$. In a mixture the surface tension σ depends on both temperature and concentration, $\sigma = \sigma_0[1 + \gamma_T\ (T - T_0) + \gamma_C\ (C - C_0)]$, where γ_T and γ_C are constants such that $q\gamma_T < 0$. In the following we measure the strength of the imposed heat flux by the flux Marangoni number $\mathrm{Ma} \equiv -qH^2\sigma_0\gamma_T/\lambda\rho\nu\kappa$, where H is the container height, λ is the thermal conductivity, ρ is the fluid density and κ is the thermal diffusivity, and the strength of the Soret effect by the Marangoni-Soret parameter $S_M = -D_S\gamma_C/D\gamma_T$, where D and D_S are the concentration and Soret diffusion coefficients. The latter quantifies the contribution to the mass flux due to temperature inhomogeneities. Thus $D_S > 0$ implies that the heavier component in the mixture migrates towards cooler regions and vice versa. As defined, Ma is positive and instability sets in as Ma increases. In pure liquids or binary mixtures with $S_M > 0$ the primary instability of the conduction state is steady state; in contrast, for sufficiently negative S_M the instability becomes oscillatory.

These results follow from equations (1)-(2) with $Gr = 0$, subject to appropriate bound-

ary conditions [1]. We impose no-slip no-mass flux boundary conditions along all rigid walls, and assume insulating boundary conditions along lateral walls ($x = \pm A_x/2$, $y = \pm A_y/2$) and a constant temperature along the bottom ($z = 0$). Along the free surface ($z = 1$) we take

$$\frac{\partial u}{\partial z} - \frac{\mathrm{Ma}}{Pr}\left(\frac{\partial T}{\partial x} + S_M \frac{\partial C}{\partial x}\right) = \frac{\partial v}{\partial z} - \frac{\mathrm{Ma}}{Pr}\left(\frac{\partial T}{\partial y} + S_M \frac{\partial C}{\partial y}\right) = w = 0, \quad \frac{\partial T}{\partial z} = \frac{\partial C}{\partial z} = 1. \tag{5}$$

The equations with these boundary conditions are invariant under the operations

$$S_x: \quad (x,y,z) \to (-x,y,z), \qquad (u,v,w,T,C) \to (-u,v,w,T,C), \tag{6}$$

$$S_y: \quad (x,y,z) \to (x,-y,z), \qquad (u,v,w,T,C) \to (u,-v,w,T,C), \tag{7}$$

generating the symmetry group D_2 of a rectangle. When $A_x = A_y$ the operation

$$\Pi_{xy}: \quad (x,y,z) \to (y,x,z), \qquad (u,v,w,T,C) \to (v,u,w,T,C) \tag{8}$$

is also a symmetry. In this case $S_y = \Pi_{xy} \circ S_x \circ \Pi_{xy}$; the two operations S_x and Π_{xy} then generate the symmetry group D_4 of a square. In either case the conduction solution $\mathbf{u} = \mathbf{0}$, $T = C = z$ is an equilibrium for all values of Ma and this equilibrium possesses the symmetry D_2 ($A_x \neq A_y$) or D_4 ($A_x = A_y$). It follows that when a steady state instability breaks the D_4 symmetry roll-like states with symmetry S_x or S_y set in at the same time as states with diagonal symmetry Π_{xy} or Π_{yx}. Theory shows that at most one of these may be stable near onset, but continuation allows us to follow these states to large amplitude. In the case of oscillatory onset theory predicts the simultaneous bifurcation from the conduction state to oscillations that are (i) invariant under the operation S_x, (ii) invariant under the operation Π_{xy} and (iii) invariant under the rotation $R \equiv S_x \circ \Pi_{xy}$ followed by evolution by a quarter period. In the following we shall refer to these states as SW, DW and RW, respectively. These acronyms stand for standing (S), diagonal (D) and rotating (R) waves (W). To compute the S_x-symmetric states we impose the symmetry $\phi(x,y,z) = \phi(-x,y,z)$ for $\phi = v,w,T,C$ together with $u(x,y,z) = -u(-x,y,z)$. The imposition of this symmetry stabilizes the SW branch against perturbations that break it and permits us to compute the SW branch using a time-integration code provided only that the SW bifurcate supercritically. Likewise to compute the Π_{xy}-symmetric states we impose the symmetry $u(x,y,z) = v(y,x,z)$, $v(x,y,z) = u(y,x,z)$ together with $\phi(x,y,z) = \phi(y,x,z)$ for $\phi = w,T,C$. There is no correspondingly simple prescription that allows us to compute the discrete rotating waves when these are unstable.

Figure 3(a) shows the bifurcation diagram when $A_x = A_y = 1.5$, $S_M = -0.01$, $\mathrm{Sc} = 100$. The figure displays the evolution with the Marangoni number of $W_M \equiv \max|w(x,y,z)|$ of the w component of the velocity $\mathbf{u}$ measured at the Gauss-Lobatto-Legendre nodes. The oscillatory instability sets in at $\mathrm{Ma} \approx 127.7$, and the three resulting solution branches all bifurcate supercritically, with the RW stable and the SW and DW unstable.

When the cross-section of the domain is perturbed by changing A_x from 1.5 to 1.51 the above picture changes dramatically (fig. 3b). The perturbation selects S_y-symmetric standing waves as the first state to bifurcate from the conduction state, followed by S_x-symmetric standing waves. The former are initially stable while the latter unstable. Thus, as in the case of steady onset ($S_M = 0$), the selected SW are oriented parallel to the *shorter* side, although exceptions can occur [2]. However, with increasing Ma the S_y-symmetric SW must transfer stability to large amplitude states (hereafter RW$'$) resembling the RW (stable in the square case), and they do so via a secondary Hopf bifurcation followed by a global bifurcation at which a hysteretic transition to larger amplitude RW$'$ takes place. Our simulations indicate that this Hopf bifurcation is supercritical and produces a secondary branch of quasiperiodic states. As Ma increases further the new frequency decreases dramatically, suggestive of an approach to a global bifurcation near Ma $= 127.37$. We surmise that this global bifurcation involves two unstable symmetry-related single frequency oscillations related to either DW or RW, but since neither of these states possesses any symmetry once the domain becomes rectangular we have no way of computing them. Note that the breaking of the D_4 symmetry 'unmasks' the supercritical SW which are unstable in the problem with full symmetry, but become stable near onset when the symmetry is broken. To confirm this interpretation of the simulations we have used the amplitudes and (nonlinear) frequencies of the three states SW, DW and RW near onset to determine the coefficients in the normal form describing the primary Hopf bifurcation. Coupled with the results of the linear stability analysis for $A_x \neq A_y$ the resulting normal form reproduces in all respects the numerical results summarised in fig. 3 [4].

In addition to the parameter regime explored above we have also carried out preliminary computations in other regimes. For example, in a square domain of side $A_x = A_y = 3$ the primary instability when $S_M = -0.05$ is an oscillatory state that does *not* break the D_4 symmetry of the container. In this case the constraints imposed by the symmetry are absent and one does not expect to find interesting transitions near onset.

This work was supported by a CNRS-Royal Society collaborative grant (AB/EK), NSF under grant DMS-0072444 (EK) and EPSRC under grant GR/R52879/01 (EK).

Reference

1. Bergeon, A., Henry, D., BenHadid, H. and Tuckerman, L. S. (1998): "Marangoni convection in binary mixtures with Soret effect", *J. Fluid Mech.*, Vol. 375, pp. 143-177.
2. Bergeon, A., Henry, D. and Knobloch, E. (2001): "Three-dimensional Marangoni-Bénard flows in square and nearly-square containers", *Phys. Fluids*, Vol. 13, pp. 92-98.
3. Bergeon, A. and Knobloch, E. (2002): "Natural doubly diffusive convection in three-dimensional enclosures", *Phys. Fluids*, Vol. 14, pp. 3233-3250.
4. Bergeon, A. and Knobloch, E. (2004): "Oscillatory Marangoni convection in binary mixtures in square and nearly square containers", *Phys. Fluids*, Vol. 16, pp. 360-372.

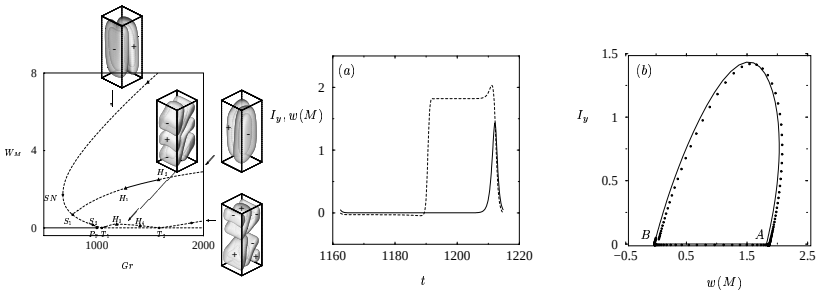

FIG. 1. (a): Bifurcation diagram for the case $N = -1$, $A_y = 1$, $A_z = 2.5$, $Pr = 1$ and $Sc = 11$, showing W_M as a function of the Grashof number Gr. Solid dots (triangles) indicate steady (Hopf) bifurcations. The insets show surfaces $w = \pm K$ for suitable choices of K at the locations indicated by the arrows. Resolution is $13 \times 13 \times 19$. (b,c):Nonlinear oscillations at $Gr = 936.5$, when $A_y = 1$, $A_z = 2.5$, $Pr = 1$ and $Sc = 11$. (b) Time evolution over one period of $I_y \equiv w(M) - w(S_y(M))$ (continuous line) and $w(M)$ (dashed line) at a generic point M. (c) Phase plane representation of the oscillation in (a). When $I_y = 0$ the solution is D_2-symmetric; when $I_y \neq 0$ it is only S_C-symmetric.

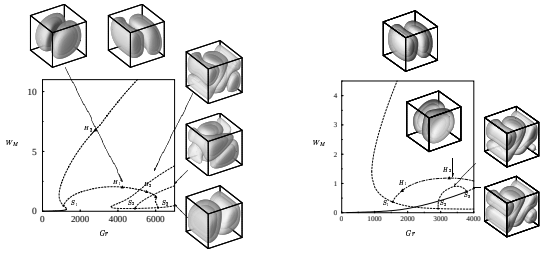

FIG. 2. As for fig. 1-a but for $A_x = A_y = 1$ and (left) $N = -0.99$, (right) $N = -1.007$. Resolution is $17 \times 17 \times 17$.

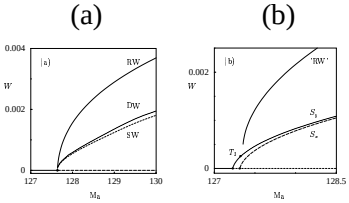

FIG. 3. Bifurcation diagram showing $W = \max_t w$ as a function of Ma for $Pr = 1$, $Sc = 100$, $S_M = -0.01$, $A_y = 1.5$ and (a); $A_x = 1.51$ (b): $A_x = 1.51$. Rotating waves are indicated by RW and standing waves by either DW or SW, depending on their symmetry. In (b), oscillations resembling rotating waves at large amplitude are indicated by 'RW' and are present for Ma ≥ 127.35. The secondary torus bifurcation T_2 occurs at Ma≈ 127.32 and the resulting two-frequency oscillations (not shown) have been observed for $127.32 \leq$ Ma ≤ 127.37